J. Condensed Matter Nucl. Sci. 21 (2016) 81–96

Research Article

Investigations of the Lugano HotCat Reactor

Mathieu Valat*, Alan Goldwater, Robert Greenyer, Robert Higgins and Ryan Hunt

Martin Fleischmann Memorial Project

Abstract

Since its release, the "Lugano Report" has attracted a lot of attention from many scientific groups as well as individuals. Following attempts to reproduce the claimed results, the Martin Fleischmann Memorial Project†(MFMP) is adding significant insights to the replication community across the Internet. The first part of the paper describes the replication of the Lugano Report's thermal measurements. It presents the experimental setup, instrumentations as well as the results produced by the MFMP team. The second part describes attempts to reproduce the excess energy claimed in the Report. After ten experiments and five incremental revisions of the apparatus, MFMP published results on the Internet showing apparent correlation between anomalous heat production and broadband low energy gamma radiation. This paper offers a review of these two significant experiments, done in March 2015 and January 2016.
 ISSN 2227-3123

Keywords: Andrea Rossi, e-cat, Lithium aluminum hydride, Lugano report, Nickel, Replication

1. Replication of the Thermal Heat Measurement from the Lugano Report

Following the release of the Lugano Report [1], the Martin Fleischmann Memorial Project (MFMP) decided to allocate part of its efforts toward replication/validation of the report's thermal measurements. Numerous shortfalls were found in the measurements and analyses within this report. One critical error was determination of the temperature based upon an emissivity function for alumina that was wrong [2], which occurred due to lack of additional means of temperature measurement for correlation. This part of the project (funded by the Infinite Energy Foundation) consisted of reverse-engineering duplication of the geometry and materials of the Lugano "HotCat" reactor and its metallic mounting rack. The objective was to produce a calibration dataset for direct comparison with the reported Lugano measurements [1].

For this calibration, Temperature of the replica reactor was measured using the same Optris PI-160 thermal imaging camera with identical factory calibration (for measurement up to 1500°C), and emissivity selection was implemented exactly as in the Lugano analyses. The calibration was performed with a sweep of electrical heater coil Power input (presumed to be equal to heat output), measured with the same power analyzer (PCE 830) as the system described in

†www.quantumheat.org.

*Corresponding author. E-mail: mathieu.valat@gmail.com.

 ISSN 2227-3123

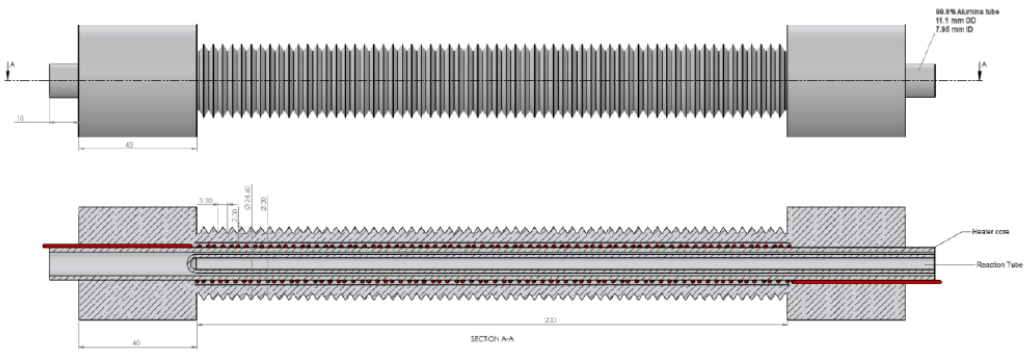

Figure 1. Schematic of the ceramic cell.

the original document. For this calibration, no fuel would be used, so the sole source of heat would be electrical input to the heater coil. The calibration based upon this replica would be used to produce a function, $T_{\mathrm{Lugano}} = f(P)$, that could be used to determine the heats generated in the Lugano experiment by direct comparison, instead of by calculation as was done in the report.

According to instructions in the Optris infrared camera manual, it was necessary to use a high-emissivity black paint on the surface of the alumina reactor to set the emissivity factor of the camera. The high-emissivity paint was provided by Aremco (reference 840-CM) for use in this test.

This experiment used additional means of temperature measurements not used in the Lugano Report. A Williamson infrared Pyrometer (model Pro 91-65-C) and type-B and type-K thermocouples were used to cross check the measurements made by infrared camera. The Williamson pyrometer was a dual-wavelength instrument that self-calibrates for emissivity based on measurement at two adjacent wavelengths. Subsequent to calibration of power, these additional measurements would relate $T_{\mathrm{actual}} = f(T_{\mathrm{Lugano}})$ to get a better idea of the correct temperatures under which the reactor was operated. This temperature mapping is not a part of the extraction of the operating heat in the Lugano experiment, but rather just supplemental information.

The HotCat replica was comprised of alumina ceramic tubing, wound with a single-phase heating coil, and with an over molded triangular fin surface having similar geometry and dimension as the Lugano device. Figure 1 shows the design dimensions. The fins described in the original report were cast over the core tube using a purpose-made two-part mold.

The fins are made with Cotronics RTC-60 castable alumina. Figure 2 shows the two reactors side by side, the Lugano apparatus and MFMP's replica, each on a scale. The weight of the replica is 20 g (4.4%) more than the original Lugano reactor.

Compared to the original experiment, the main variation was the heating element. The maximum design power of 1.9 kW and 1400°C peak temperature was inferred in the Report, but the metallic composition of the heater coil was not described. The MFMP replica (aka "Dogbone") used Kanthal A1 wire, rated to 1400°C for short intervals. Since the aim of this experiment was not to create excess energy but rather to verify the thermal measurements, only a source of Joule heating was provided. Therefore, no attempt was made to duplicate the triple coil winding and three-phase power used in the Lugano apparatus. While this sounds like a big difference, the close wound heater coil is an internal heat source that can be modeled in either case as a distributed cylindrical sheet of heat emission. The primary vector for heat loss from the apparatus is the finned exterior surface of the central tube. Particularly at lower temperatures, the finned exterior of the reactor can be modeled as having a thermal resistance to ambient and the temperature of the

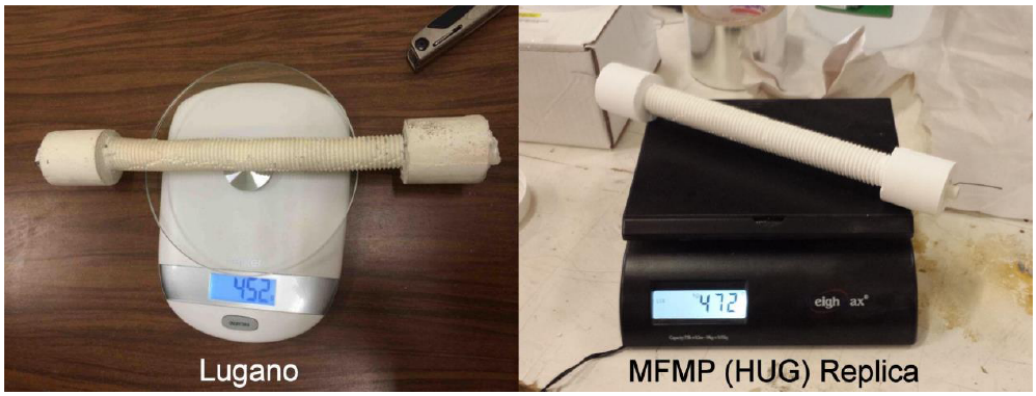

Figure 2. Photos of the original reactor and its replica.

finned surface is determined by how much heat traverses this path, not by how the power was created. Some error can be attributed to the unknown differences in radiation between the Lugano apparatus and the MFMP replica caused by possibly different temperatures inside the body and possible differences in spectral transparency of the cast alumina. Figure 3 shows the schematics of the heater coil geometry.

Thermal measurements were made up to 900 W power input – commensurate with the power given in the Lugano Report for the first part of that experiment. The thermocouples showed a maximum temperature of 843°C, compare to 975°C given by the Williamson pyrometer and an average of 971°C by the Optris infrared camera with emissivity set to 0.95.

Further measurements showed significant temperature gradient on the tube circumference and along the surface profile of the outer fins. This surface temperature variation, combined with the limited contact patch of the thermocouple beads, was probably the cause of the lower thermocouple readings compared to the pyrometer. Figure 4 shows the thermocouple attachment to the fin structure. The yellow spot was from the pyrometer aiming laser.

While this temperature gradient vertically across the finned central tube would present a problem for attempted calculation of emitted heat, the Optris camera was setup to measure an average from top to bottom and left to right in square regions along the tube. As long as the replications matched the average temperatures recorded by the Optris camera in these regions, a thermal state match between the replica and the Lugano experiment would be assumed.

The team evaluated the calibration setting of the Optris infrared camera on a paint spot with known emissivity. A value of $\varepsilon = 0.95$ was then derived iteratively for the cast material by temperature correlation between the painted spot and the immediate close proximity bare alumina. The Williamson pyrometer confirmed this emissivity within a 2% range. This also agreed with the suggested value in the Optris manual for alumina.

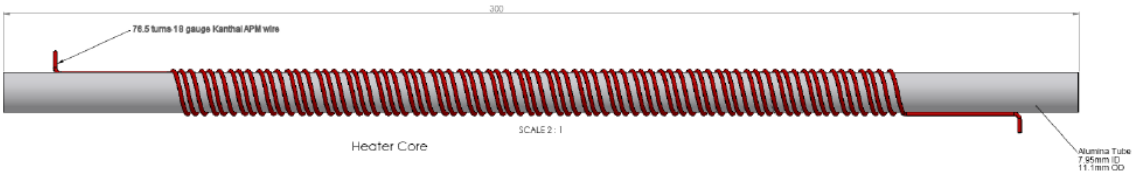

Figure 3. Schematics of the heater coil geometry.

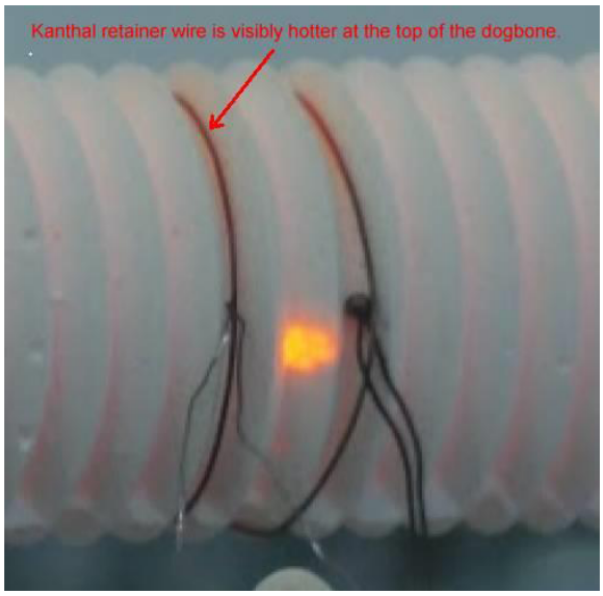

Figure 4. Thermocouple attachment to MFMP replica. Type-B on left, type-K on right.

Since alumina changes transparency in this temperature region [3], the radiant heat emitted by the heater coil through the semi-transparent material would not have had a blackbody spectrum. It would be difficult (perhaps impossible) to determine the actual thermal emission without measurement of the emitted spectrum over an optical band extending from UV to far infrared. This spectral data was not supplied in the Lugano report.

The Lugano report also did not provide $T_{\text{surface}} = f(P)$ calibration data over the entire range of power that was used during the fueled test. So the replication strategy was to create a dummy experiment to acquire the missing $T_{\text{Lugano}} = f(P)$ data to provide a means to extract how much power would have been required to reach each "Lugano thermal state". By testing with the Optris camera, it was found that if the camera remained set with an emissivity of 0.95 for data gathering, the temperature at any other emissivity could be calculated as

$$T' = T_{0.95} \sqrt[3]{\frac{0.95}{\varepsilon'}}.$$

The relation above was verified with a data point taken with the Optris camera having the emissivity manually set to $\varepsilon = 0.95$, and then to $\varepsilon = 0.45$. Thus, these temperatures were calculated in the same manner as used in Lugano report – iterated for consistency with the emissivity curve [1] (Plot 1) used in the Lugano analyses.

With a means to obtain the thermal state for the MFMP replica in direct correspondence with the Lugano data, the MFMP replica heater input power was swept while Optris thermal data was acquired. This data would provide a means to directly extract the power needed for each of the reported Lugano reaction thermal states, as if the Lugano experiment had first been run with a widely ranging power sweep in its dummy run.

Having such $T = f(P)$ data completely obviates the need for calculation of emitted heat via convection and radiation (which were found likely in error for not having included the alumina's spectral transparency). For this paper, the swept $T = f(P)$ curve of the MFMP replica was used to directly assess possible excess power in the Lugano experiment.

Unfortunately, while taking readings at 900 W input, the MFMP Optris camera was damaged by an accidental electrical short circuit. Because of this, data for input powers above 900 W are estimated via analytic curve fit extrapolations. These analyses are described in Section 2.

2. Analysis and Interpretation of the Replication Against the Lugano Test

The Lugano experimenters used an average temperature for each zone defined along the length of the ceramic apparatus. To match these values with the MFMP replica, it is necessary to match values of identical zones from both data sets. Using zones 5–9 of each apparatus allowed a very close match of both average and standard deviation values of the original Lugano calibrations. Hence, the average of these zone temperatures is used as a common thermal state to compare the values measured for the MFMP replica to those measured for the Lugano reactor. Figure 5 shows a plot of the MFMP replica data using the average from zone 5 to 9 to calculate the temperature, along with a curve fit for the data, and the corresponding iteratively calculated temperature as would have been recorded by the Lugano researchers for this experiment.

The Lugano experimenters reported their results as "Files" for sample data sets. An example for the first phase of excess heat production is File-4 reactor temperature of 1257.21°C ([1], Table 6), at an input power of 790.69 W ([1], Table 7). Using interpolation in the MFMP replica curve of Fig. 5, direct heater electrical input would have produced this same Lugano thermal state with a power input of 893.6 W. Since the fueled Lugano reactor reached this thermal state with an input of only 790.69 W, an apparent excess heat of 102.9 W is indicated from the reaction. The corresponding "actual" surface temperature for this reaction is estimated as 944°C and the apparent coefficient of performance (COP) is 1.13.

After running the experiment at this input power for 10 days, the Lugano experimenters increased the input power

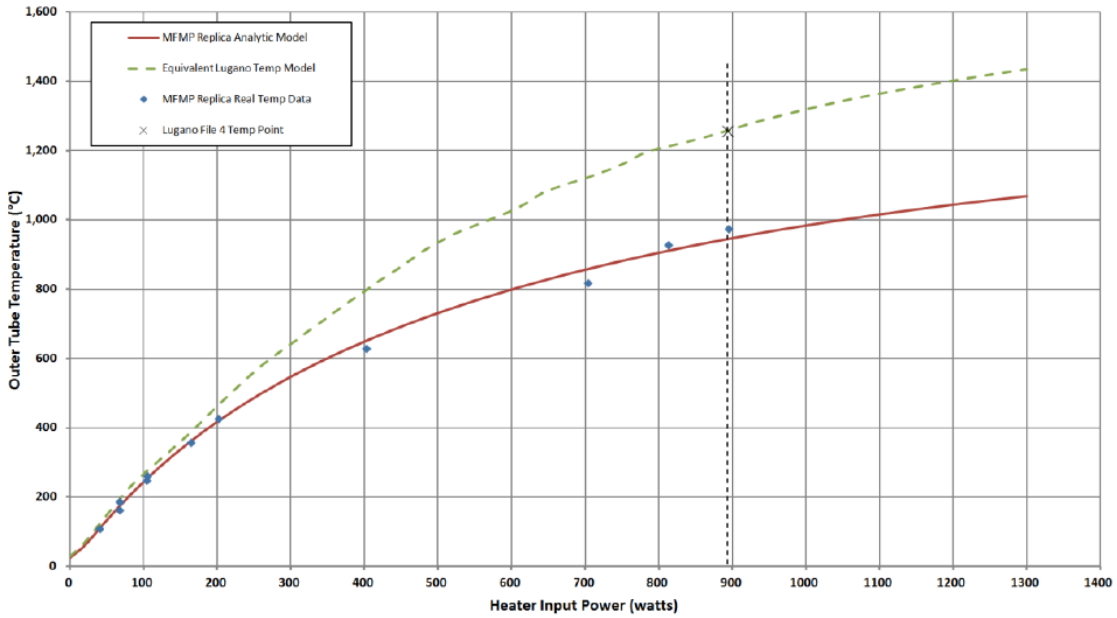

Figure 5. Graphical extrapolation of our measurement.

for a new, higher temperature reaction state. The data from this state was examined in a similar manner. In the Lugano File-8 data, the reactor surface temperature was reported as 1404.04°C using an input heater power of 918.24 W. Using extrapolation with the fitted curve in the MFMP replica, the replica would have reached this Lugano thermal state with a direct heater input of 1208 W. The apparent excess heat is estimated as 289.8 W with an apparent COP of 1.32, at an operating "actual" surface temperature of 1045°C. Complete calculations and original plots are available for public download[a].

Note that the temperatures reported are surface temperatures, and the core temperature is likely 150–200°C hotter. The apparent excess heats, COPs, corresponding "real" temperatures, and excess heat variation with temperature seem commensurate with reports from similar experiments [4,5]; and in the case of A. Parkhomov [4], excess heat was assessed via mass-flow calorimetry.

As an additional correlation, an attempt was made to apply the same analysis to the dummy run data from the Lugano report ([1], Section 5). The Lugano experimenters based the veracity of their analyses upon the dummy run data. With an electrical input of 479 W, the reported average temperature was 442.5°C. Interpolating Fig. 5 MFMP replica data, this Lugano thermal state should have been achieved with a heater input power of only 190.6 W. The dummy run data appears to be truly anomalous. According to the thermal response of the MFMP replica, the 479 W input should have produced an "actual" surface temperature of 715°C and a corresponding iterated Lugano-technique temperature of 914°C. How could the measured Lugano dummy run temperature have been so low? If the Optris temperature measurement was the same as subsequent fueled runs, the input heater power should have been 190.6 W, not 479 W (an error of 251%). If the electrical power for the dummy run was measured accurately, the Optris camera should have measured an iterated Lugano-technique temperature of 909°C instead of 442.5°C. Since the dummy run was conducted before fueling the reactor, the system would have been electrically disassembled, fueled, and then reassembled. It may be speculated that there was a mistake in the original dummy run electrical connection or measurement, that was unknowingly corrected during the reassembly, prior to making subsequent fueled runs.

Additional analyses of the MFMP replica data, as applied to the Lugano results, showed that if the single, hottest zone (8) of the MFMP replica was used as the basis for comparison, instead of the zones 5–9 average of Fig. 5, less excess power is estimated. Hottest zone analysis estimates the lowest excess heats File-4 excess heat of 63.3 W, and File-8 excess heat of 220.8 W.

In summary, based upon analyses using the MFMP replica "Dogbone" data, the Lugano experiment is estimated to have produced at least an order of magnitude lower excess heat than reported. However, excess heat is not ruled out commensurate with that seen by other experimenters using a similar LENR technology [4,5]. Also, the MFMP replica data suggests that an anomalous error occurred during measurement of the Lugano dummy run.

3. Introduction to the Glowstick Experiments

MFMP member, Alan Goldwater, further investigated the thermal behavior of Lugano-like systems. The new Glowstick design retains important features from the Lugano apparatus, but techniques were developed to allow reuse of the reactor over multiple experiments, and to provide a simultaneous experimental control. Several initial tests explored the operational range of power, temperature and refractory materials. A series of incremental experiments further refined the mechanical and control systems, yielding a robust and stable experimental platform built from readily available components, expanding further replications within the community.

[a]"Dogbone Analysis of Excess Heat" http://goo.gl/0rP40x

4. Description of the Reactor Geometry and Materials

The fifth iteration of the Glowstick design used a mullite ceramic tube as the main reactor body. The fuel was loaded into a stainless steel capsule, then inserted into the reactor body. Figure 6 shows the geometry and dimensions of each element. Both ends of the reactor were tightly sealed on a polished surface of the mullite tube using Swagelok fittings with aluminum compression ferrules. This technique provided connection of the reactor to industry-standard gas and vacuum plumbing, with easy assembly.

The Swagelok sealing technique was repeatable and was proven to be hydrogen-tight at reactor core temperatures up to 1300°C. This was important because vacuum degassing and control of hydrogen pressure were thought to be necessary for loading of hydrogen into nickel, and for subsequent reaction processes.

The fuel was comprised of nickel (Hunter Chemical AH50, particle size $4.5 \simeq 1.5$ μm), lithium tetra-hydro-aluminate (henceforth referred to as LAH or $LiAlH_4$ in formulae) (Sigma Aldrich, CAS 16853-85-3) and micro-encapsulated lithium (Nanoshel, CAS 7439-93-2) mixed under argon atmosphere with a mortar and pestle to reduce the LAH particle size and provide a homogeneous fuel mixture. The fuel mixture was then placed in a stainless steel capsule and closed with a vented set screw. The null capsule was identical to the fueled capsule but filled instead with alumina powder.

The heater element was a single phase coil made of Kanthal A1 wire (18 AWG = 1.02 mm). The coil was divided exactly in half, so that the active and null sides of the cell each receive one half of the applied Joule heating power. Each coil had an alumina cover tube to provide thermal insulation and support for identical type-K thermocouples.

A manifold enabled the inside chamber of the reactor to be vacuumed, vented and pressurized with hydrogen gas. To reduce the dead volume in the reactor chamber, the empty parts were filled with alumina or stainless steel rods. A two-stage vacuum pump (Welch Duo-Seal 1400) with Pirani gauge was used for initial degassing and bake-out of the reactor to 5 Pa or less (at the gauge). The micrometer metering valve was subsequently used to bleed excess hydrogen into a vacuum reservoir.

An alumina felt plug at the center of the reactor was used in an attempt to provide a physical barrier to liquid

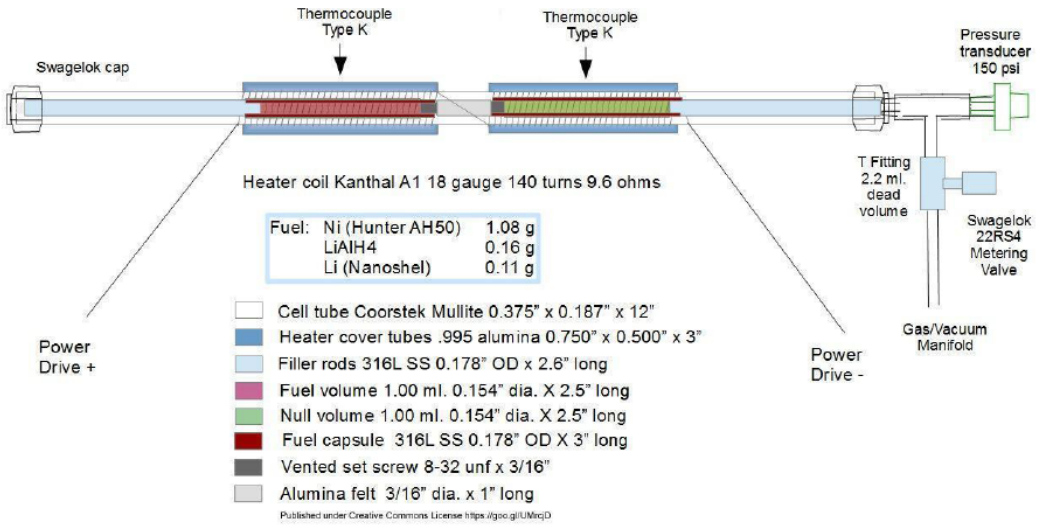

Figure 6. Details on the geometry of the Glowstick GS5 reactor.

lithium migration, while giving sufficient permeability to allow vacuum and hydrogen pressure to reach the active fuel capsule. This showed to be a partially effective barrier.

5. Description of the Control System

A closed loop design allowed the system temperature to be constantly controlled over the duration of the experiment. Control was provided by a PID controller (Dwyer model 16868) with type-K thermocouple in contact with the reactor on the fueled side, and an SCR proportional phase angle power controller (CCI model 1022). The heater power leads were fed through a Tektronix model PA1000 power analyzer, providing RMS power data stored at two samples per second intervals. The PID controller could be programmed for ramp/soak temperature sequence, or bypassed for manual control.

Two thermocouples (type-K) and a Honeywell 0–150 psia pressure sensor were connected to a 16 bit ADC DAQ (HUGnetLab model E) for collection and Internet broadcasting of temperature and pressure data in real-time.

A gamma spectrometer (Spectrum Techniques UCS-30, 38 $\times$ 38 mm cylindrical PAXON PX NaI+Tl scintillator) monitored gamma radiation coming from the reactor, with a MCA range of $\simeq$20 keV–1.5 MeV. The scintillator head was surrounded by $\simeq$100 mm of lead on all sides (240 kg) to suppress background. A 50 $\times$ 50 mm aperture admitted radiation from the active fuel part of the reactor, over a solid angle of about one steradian. A Geiger-Muller counter (GQ Electronics model GMC-320+) provided cross-check in the 300 keV–3 MeV range.

It is important to note for future replications that the heater power must be transformer isolated from the mains supply. Additionally, a 5 mA triggered GFCI (ground fault circuit interrupter) should be used as shown in Fig. 7, to avoid damage to the DAQ equipment from heater electrical leakage through the hot ceramic reactor assembly. In earlier experiments it was found that at temperatures approaching 1000°C, Glowstick mullite and alumina reactor tubes became electrically conductive. As a result, heater power was causing common mode noise currents in thermocouple

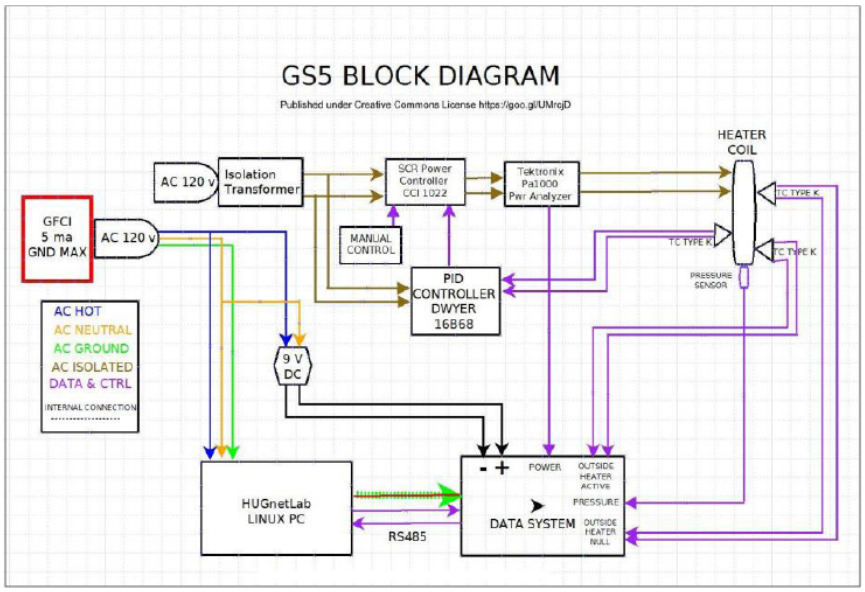

Figure 7. Schematic of the data acquisition and control system.

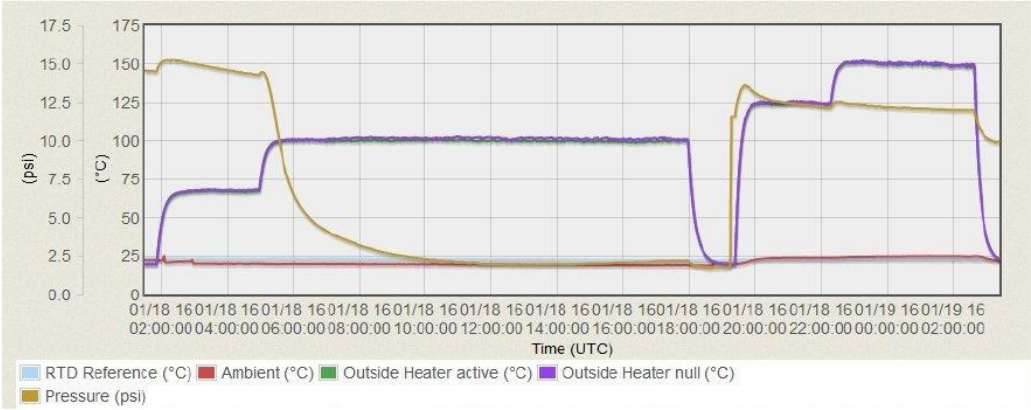

Figure 8. Evidence of hydrogen loading into the fuel.

junctions in contact with the ceramic. Changes to the experimental setup were then made to mitigate the effect of such induced current[b].

6. Pre-processing of the Nickel Powder

The nickel powder was baked before mixing the fuel together. The reasoning was that repeated thermal oxidation and reduction of the Ni particle surface may aid in creating cracks and increased surface area. The resulting micro-scale cavities and lattice flaws are thought essential for deep loading of hydrogen.

Consequently, two cycles of – baking the nickel powder at 200°C in a furnace were applied, followed by heating under continuous vacuum at 115°C for several hours to remove trace water vapor that might be adsorbed by the nickel and other cell contents.

A separate test run prior to adding other fuel components was done to evaluate loading of hydrogen following pre-processing. For this test, the baked nickel powder alone was placed in a stainless steel fuel capsule and installed in the reactor. After sealing, the reactor was evacuated and hydrogen was added from a gas cylinder to 1 bar absolute pressure.

As shown in in Fig. 8, the cell pressure (yellow trace) declined from 1 to 0.2 bar during five hours at just over the 100°C set point, corresponding to about 120°C in the fuel capsule.

Following the loading test, the fuel capsule was removed from the reactor, sealed with tape and stored in ambient air for several days. The capsule was then placed in a glove bag along with other fuel components. The nickel was removed from the capsule under Argon cover gas and mixed with the other ingredients before loading back into the fuel capsule.

7. On LAH Breakdown and Interactions with Nickel

Because variations of hydrogen pressure is an important experimental evidence to support adsorption/absorption of hydrogen inside the metal lattice, it is proposed to recall some mainstream reference first, to draw the picture of LAH breakdown during the course of our experiments.

[b]"Glowstick Thermocouple Ground Leakage" http://goo.gl/V8gz6c

Andreasen et al. [6] detail the first states of dehydrogenation of this compound as follow.

$$\begin{array}{llll} 150 < T < 175°C, & 3LiAlH_4 & \rightarrow & Li_3AlH_6 + 2Al + 3H_2, \quad 5.3\ \text{wt.\%}\ H_2, \\ 180 < T < 220°C, & Li_3AlH_6 + 2Al & \rightarrow & 3LiH + 3Al + \frac{3}{2}H_2, \quad 2.6\ \text{wt.\%}\ H_2, \\ T > 400°C, & 3LiH + 3Al & \rightarrow & 3LiAl + \frac{3}{2}H_2, \quad 2.6\ \text{wt.\%}\ H_2. \end{array}$$

The first steps are interesting because it enables hydrogen exposure of nickel powder around its Debye temperature. Wiench et al. [7] showed evidence of multiple pathways during the thermal decomposition of the LAH compound using MAS and MNR spectroscopy, including the following.

$$20°C < T < 150°C, \qquad LiAlH_4 \rightarrow LiH + Al + \frac{3}{2}H_2, \quad \text{among other pathways.}$$

Jain et al. [8] expanded his reviews to multiple complex hydride compounds and provided additional evidence to the diversity of breakdown paths these hydrides are able to follow.

Most of the studies were done for the purpose of hydrogen storage technology, hence limiting temperature range to 400°C. However Lin et al. [9] calculated from experimental evidence the solubility of hydrogen in lithium aluminum compounds up to 1200 K, showing a high value of solubility, increasing as lithium content increases.

Interesting behavior has been ascribed to the interaction of the electronic shells of nickel and hydrogen anions (H^-), also called protide. Descriptions of the involvement of this less common state of hydrogen are provided in these publications [10,11].

$$\begin{array}{llll} T \simeq 500°C, & 2\ LiH + 2\ Al & \rightarrow & 2\ LiAl + H_2 \quad \text{(reversible)}, \\ T \simeq 688.7°C, & LiH\ (\text{solid}) & \rightarrow & [Li^+ + H^-] \quad \text{(liquid, ionic hydride)}, \\ T > 850°C, & 2\ [Li^+ + H^-] & \rightarrow & 2\ Li + H_2. \end{array}$$

While very little is available in the literature on this particular state of hydrogen, it is interesting to observe that liquid LiH is an ionic hydride and the hydrogen exists in solution as hydrogen anions. In addition, Kasagi et al. [12] showed cross section capture of low energy proton or deuterons on lithium is greater when Lithium is in a dense ionic state.

Scanning Electron Micrographs (SEMs) and corresponding EDS-X analyses provided by Edmund Storms from Kiva-Labs and Sangho Bok from University of Missouri aided in understanding the behavior of this chemical system at high temperature. Note the similarity of the micrograph of Fig. 9 to the one of the ash produced for the Lugano report ([1], Appendix 3, Fig. 2). Figure 9 suggests that, once molten, the Li–Al–H alloy wets to the oxide-free Ni powder.

However, the surface of the spiky Mond process Ni particles (obtained from nickel tetracarbonyl) is complex on both the micro-scale and the nano-scale. In some places the molten Li–Al–H (an ionic hydride) may be in direct contact with the Ni surface. In other places, due to the surface tension of the liquid metal, surface complexity may be "skinned over", leaving micro-scale and nano-scale voids. If the Ni+LAH system proves to be LENR active, this

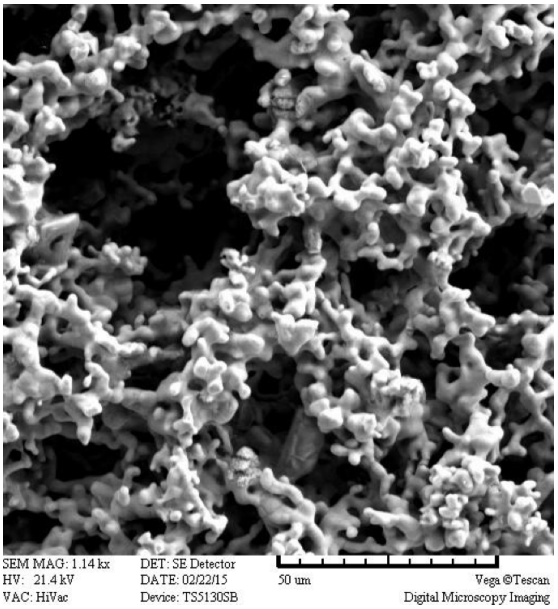

Figure 9. SEM picture of the powder wetted by the LAH after high temperature migration (courtesy of Kiva-Labs).

Li–Al–H ionic hydride interface to the Ni should be the subject of extended study. References possibly pertinent to such a study have been included [13–15].

8. Operating Parameters

After the experimental setup was assembled and all instruments connected and calibrated, the reactor tube was vacuumed for two hours and left overnight. Temperature was increased to just over 100°C. The partial dissociation of the LAH compound slowly produced an increase of pressure. The flux of hydrogen generated by this increase of temperature would have reduced any remaining nickel oxides, leaving a clean surface on the metal particles. Further vacuum to under 100 Pa absolute pressure was then applied to remove resulting trace water vapor.

The in-situ oxide removal was followed by raising the core temperature to 122°C, deliberately below the lowest known Debye temperature (132.85°C) [16] of nickel where it was held for over 6 h before raising the temperature to comfortably below the nickel Curie temperature (358°C). During this entire period hydrogen evolved from the LAH, so a bleeder valve was adjusted manually to keep the reactor pressure at 1 bar or less.

Next, the reactor core was slowly cooled down to a temperature comfortably above the maximum Debye temperature of nickel (204°C). Afterward, the temperature was quickly increased to 400°C (above the nickel Curie temperature).

Following an extended dwell to allow completion of the first phase of LAH decomposition, the temperature was increased in several steps to $\simeq$700°C, where additional phase change was expected to occur. A further increase to above 900°C put the LAH into a state of reversible release of hydrogen.

After additional dwell time to watch pressure behavior, thermal cycling was started, alternating between 600 and 1000 W RMS input (yielding from $\simeq$900°C to $\simeq$1200°C) at 30 min intervals, and continuing for several hours. During this period, an apparent increase in temperature differential between the active and control sections to $\simeq$50°C was

observed as shown in Fig. 10. Compared against calibrations, the power difference was assessed to about 70 W greater heat from the fueled section, corresponding to a COP of 1.09. This COP is small, and when compared to possible thermocouple aging and other sources of measurement error, may prove to be borderline for a claim of excess heat.

9. Radiation Measurements and Analysis

As previously mentioned, this experiment was monitored with an NaI–Tl scintillator attached to a UCS-30 spectrometer with the scintillator placed 33 cm away from the fuel and shielded within a lead cave. Integrations were started manually back-to-back, but over somewhat irregular period lengths. Overall, 24 integrations were made over the course of the experiment from cold reactor to cold reactor. During one 4-hour integration period highlighted in Fig. 10 as "Spectrum 7"), a broadband X-ray/gamma emission (10–400 keV) was recorded.

The curve shape of Spectrum 7 was consistent with Bremsstrahlung radiation as shown in Fig. 11. This spectrum is the longest of the series (a 4 h integration). The signal captured has nearly an order of magnitude amplitude above average levels seen in the other spectra.

Figure 12 shows a photometric background spectrum that was extracted from Spectrum 1 and Spectrum 24 ; cases where no reaction should be present.

When the background spectrum of Fig. 12 is applied to Spectrum 6, a case also expected to be null, the residual shown in Fig. 13 is obtained. As can be seen in this linear plot, the residual is zero mean over the bulk of the valid spectrum. The noise increase seen below 200 keV is due to the Poisson noise characteristic of a random source (similar to noise in astronomical photometry), wherein the noise increases as the square root of signal strength.

Photometric reduction of the actual data comprised energy resampling of the source data spectrum to a calibrated 1 keV per sample energy scale, and subtraction of a background scaled by the total length of live time of the source spectrum data.

Figure 14 shows the radiation signal spectrum for Spectrum 7 with photometric calibration.

This data was intensely analyzed by the crowd (internet observers), to see if it could be an artifact of measurement error or contamination. Possibilities including a cosmic ray burst, radon concentration and radio-frequency interference were proposed, tested and disproved. Figure 15 shows the results of radon investigation.

Replication and further experimental evidence is necessary with complementary equipment to define the origin of this signal. The complete analysis is available for further study [17].

No radiation signal above background was detected by the GMC320+ Geiger-Muller counter during this time.

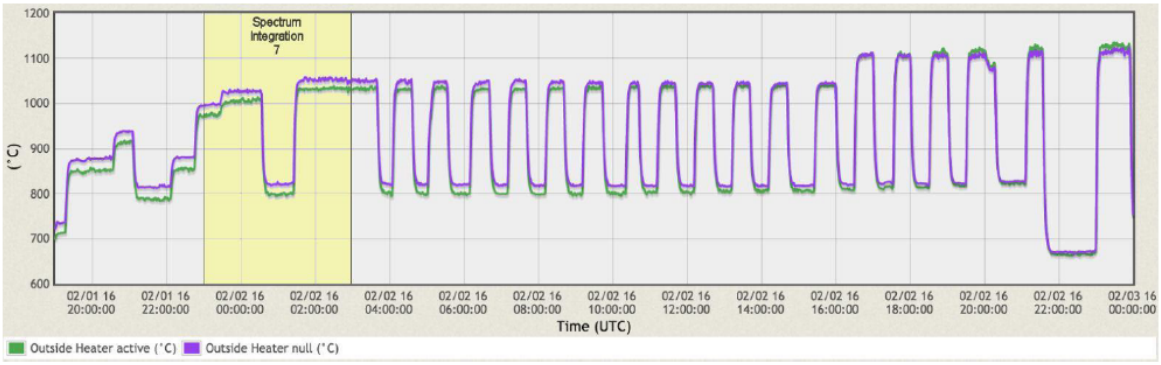

Figure 10. Increase of temperature on the fueled side.

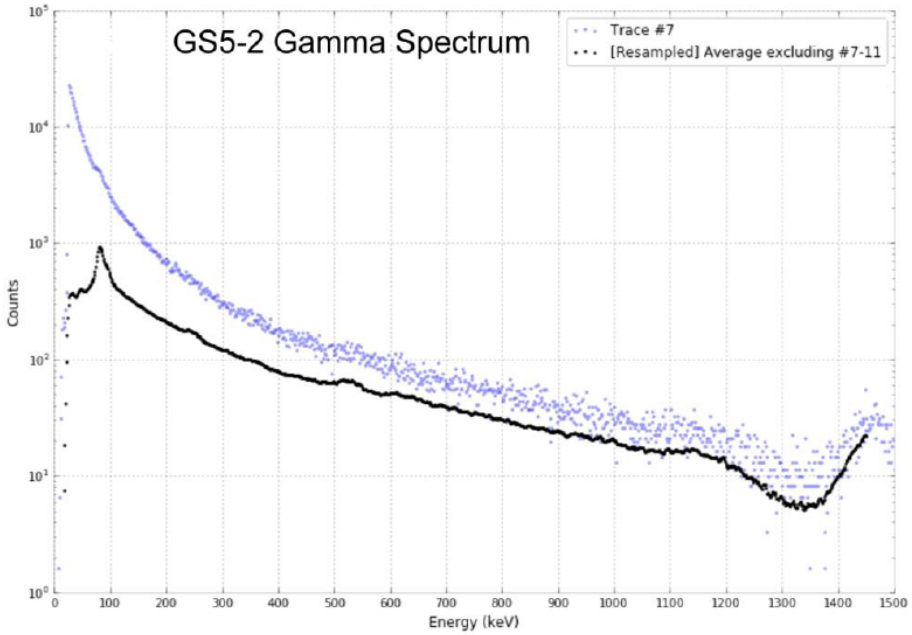

Figure 11. Gamma radiation at the beginning of the anomalous heat period compared to normalized background.

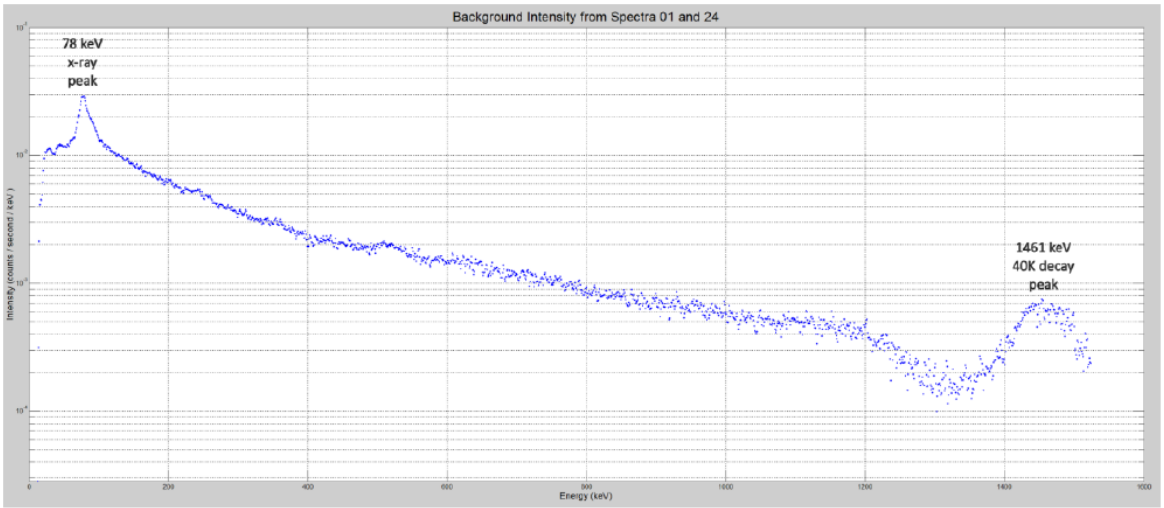

Figure 12. Photometrically calibrated background spectrum.

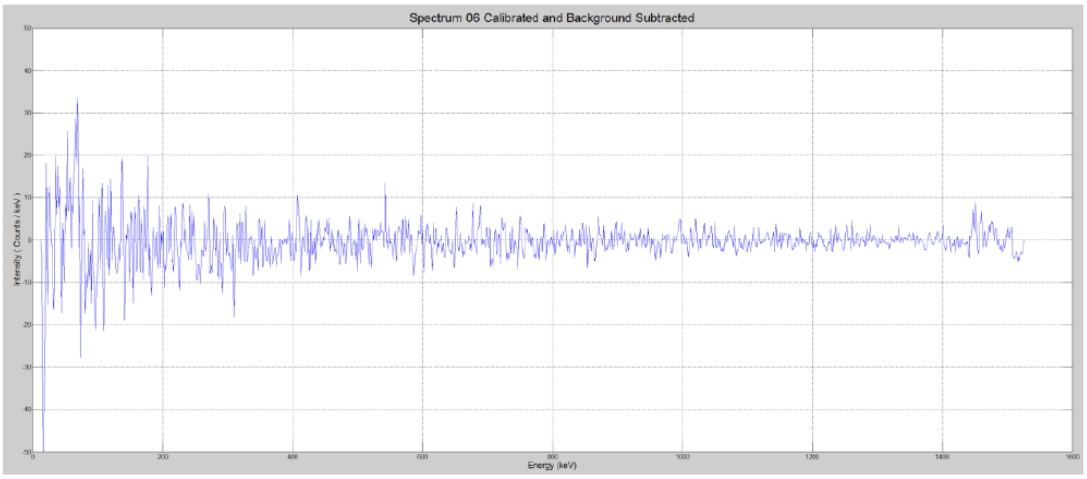

Figure 13. Null Spectrum #06 residual from background subtraction.

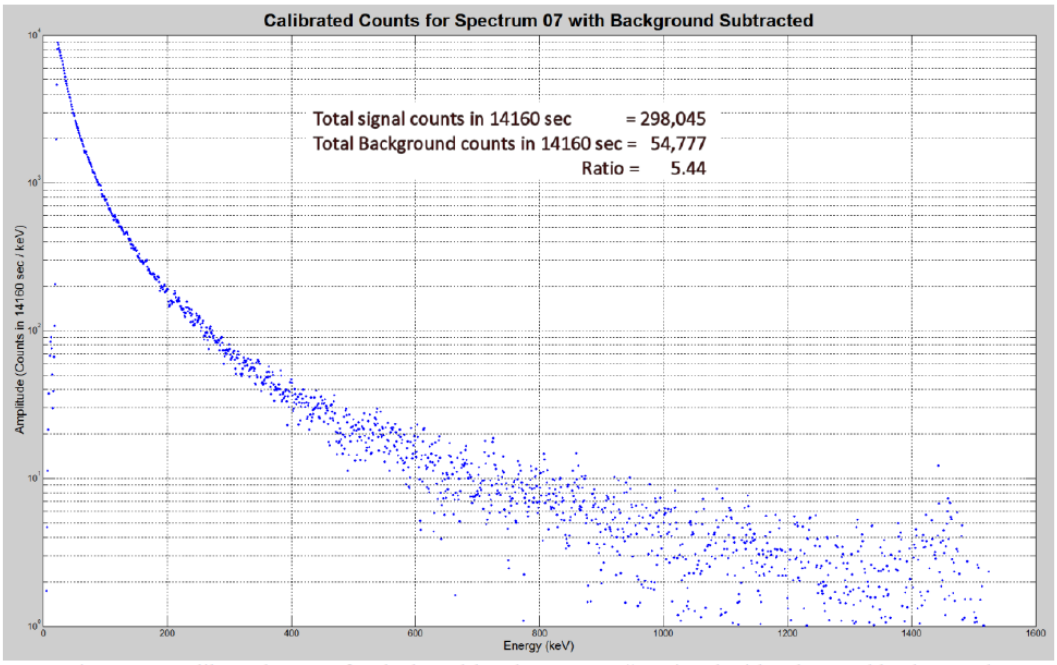

Figure 14. Calibrated counts for the broad-band Spectrum #07 signal with subtracted background.

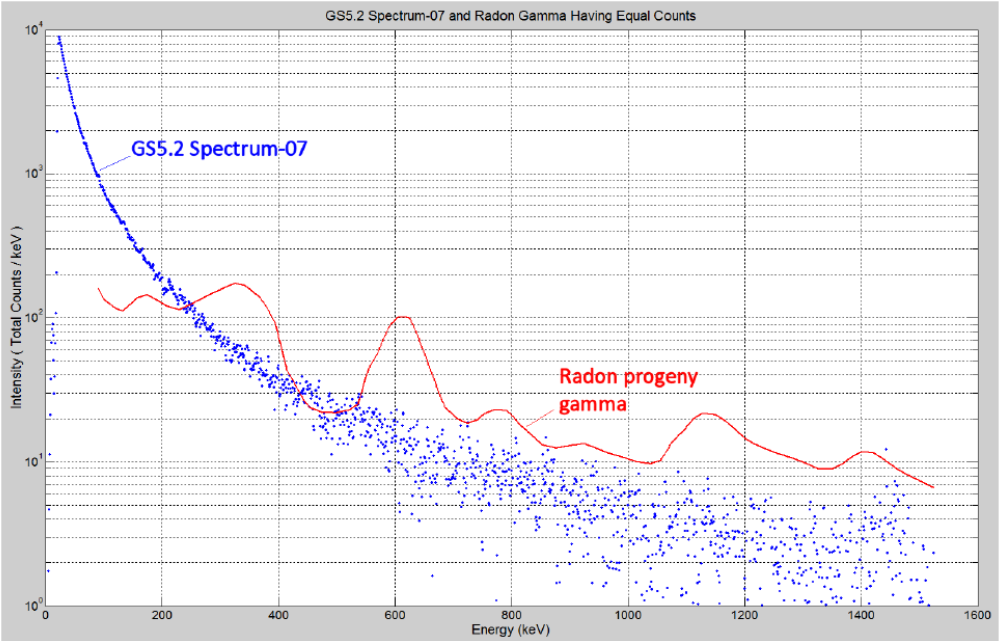

Figure 15. Broadband spectrum compared to typical radon spectrum.

It should be noted that this is an inexpensive instrument with poor sensitivity, especially to low-energy (<100 keV) gamma radiation. Post experiment testing of the GMC320+ and modeling with the spectrum detected by the scintillator suggested the GMC320+ should only have seen a small number of counts above background. Depending upon the unknown time spread of the scintillator detected signal (up to 4 h), this may not have been discernable above the background counts in the GMC320+.

10. Conclusion

With a diligent scientific study of claims made for Rossi's HotCat reactor, the MFMP team has provided evidence of an overestimation of the results in the Lugano report.

The incorrect setting of the emissivity parameter by a large margin shows how the Lugano team overestimated the thermal output of the HotCat reactor in analyses subsequent to the Lugano test. However, the added MFMP replica data and its co-analysis with the Lugano data cannot disprove a smaller effect, as interpolated/extrapolated in this paper.

Using the Glowstick reactor in its 5.2 iteration, MFMP showed in Live Open Science, that a small amount of excess thermal energy and a gamma photon spectrum were generated by a system using heated nickel, lithium and hydrogen. Additional iterations are being developed by the MFMP group to provide improved evidence of results and increased performance.

The lack of information disclosed by Leonardo Corporation make the replication task difficult. However, MFMP has gathered enough know-how and data from public domain reports to search for evidence of a genuine effect. Even though the nature of the phenomenon is still open to debate, the results compel additional efforts.

From an industrialist point of view, the (currently) small effect provides little hope for short term commercial emergence of this new phenomenon. However, this rather small effect should be a priority for public scientific investigation.It is important to assess the nature of the phenomenon and determine its possible future impact to the world's energy portfolio.

Acknowledgements

This work is dedicated in memoriam to Pr. Martin Fleischmann. It has been enabled by the generous financial, workforce and support help that was provided over the years by the contributors of the Martin Fleischmann Memorial Project. We offer them our best thanks.

References

[1] G. Levi, F. Evelyn, H. Bo, P. Roland, T. Lars and E. Hanno, Observation of abundant heat production from a reactor device and of isotopic changes in the fuel, http://ecat.com/wp-content/uploads/2014/10/ECAT-test-report-2014.pdf, October 2014.
[2] Bob Higgins, Making sense of alumina spectral emissivity (2015). Download link http://goo.gl/a91xbm.
[3] O. Rozenbaum et al., A spectroscopic method to measure the spectral emissivity of semi-transparent materials up to high temperature, *Rev. Sci. Instr*. **70**(10) (1999) 4020–4025.
[4] A.G. Parkhomov, Long- term tests of the nickel – hydrogen reactor with flow calorimeter, in *the proc. 23rd Russian Conf. on Cold Nuclear Transmutation of Chemical Elements and Ball Lightning* (2016), submitted.
[5] Zhang Hang, Test of abnormal heat in hydrogen loaded metal – Report 2 (2016). Download link http://goo.gl/VjXaNf.
[6] A. Andreasen, T. Vegge and Allan Schrøder Pedersen, Dehydrogenation kinetics of as-received and ball-milled LiAlH4, *J. Solid State Chem.* **178**(12) (2005) 3672–3678.
[7] J.W. Wiench, V.P. Balema, V.K. Pecharsky and M. Pruskia, Solid-state 27 Al NMR investigation of thermal decomposition of LiAlH 4, *J. Solid State Chem.* **177**(3) (2004) 648–653.
[8] I.P. Jain, Pragya Jain and Ankur Jain, Novel hydrogen storage materials a review of lightweight complex hydrides, *J. Alloys Compounds* **503**(2) (2010) 303–339.
[9] R.Y. Lin and M. Hoch, The solubility of hydrogen in molten aluminum alloys, *Metallurgical Trans.* A **20**(9) (1989) 1785–1791.
[10] Z.P. Li, B.H. Liu, K. Arai, N. Morigazaki and S. Suda, Protide compounds in hydrogen storage systems, *J. Alloys Compounds* **356** (2003) 469–474.
[11] Çakanyıldırım, Çetin, and Metin Gürü, Hydrogen cycle with sodium borohydride, *Int. J. Hydrogen Energy* **33**(17) (2008) 4634–4639.
[12] J. Kasagi and H. Yonemura, Ionic Debye screening in dense liquid plasmas observed for Li+ p, d reactions with liquid Li target, *Nucl. Phys. Rev.* **26 (**Suppl) (2009) 44–48.
[13] S. Focardi, R. Habel and F. Piantelli, Anomalous heat production in Ni–H systems, *Il Nuovo Cimento A* (1971–1996) **107**(1) (1994) 163–167.
[14] E.G. Campari,, S. Focardi, V. Gabbani, V. Montalbano, F. Piantelli and S. Veronesi, Overview of H–Ni systems old experiments and new setup, *5th Asti Workshop on Anomalies in Hydrogen/Deuterium loaded Metals* (2004).
[15] J.J. Dufour, X.J.C. Dufour and J.D. Vinko, Pico-chemistry the possibility of new phases in some hydrogen/metal systems, *Int. J. Modern Phys.* B **27**(15) (2013) 1362038.
[16] Yu M. Kagan and I.S. Lyubutin, *Applications of the Mössbauer Effect Applications in other Fields*, Vol. 5, CRC Press, Tokyo, 1985, p. 1394.
[17] Bob Higgins, Iceberg in the Glowstick 5.2 Data (2016). Download link http://goo.gl/DOiXYe.